ORIGINAL ARTICLE

Medical Journal of Western Black Sea
Batı Karadeniz Tıp Dergisi

Med J West Black Sea 2026; Early View
DOI: 10.29058/mjwbs.1822432

In-silico engineering of an antimicrobial growth factor fusion protein to prevent post-laser infection in hemorrhoidal wounds

Hemoroidal yaralarda lazer sonrası enfeksiyonu önlemek için antimikrobiyal büyüme faktörü füzyon proteinlerinin bilgisayar simülasyonlu tasarımı

Özlem Karaca Ocak[1], **Zoha Naeem**[2]

[1]Üsküdar University Faculty of Medicine, Department of General Surgery, İstanbul, Türkiye
[2]University of Central Punjab, Faculty of Biotechnology, Department of Bioinformatics, Lahore, Pakistan

Cite this article as: *Karaca Ocak Ö and Naeem Z. In-silico engineering of an antimicrobial growth factor fusion protein to prevent post-laser infection in hemorrhoidal wounds. Med J West Black Sea. 2026; Early View.*

ABSTRACT

Aim: Post laser wound infection is a recurrent complication after hemorrhoidal surgery mainly because polymicrobial flora is colonized in the anorectal environment and the mucosal repair is impaired. This study aims to overcome the drawbacks of current therapeutic options and to provide a novel generation of prophylactic biomolecule with antimicrobial activities, monitored to meet the specific conditions of the microenvironment of anorectal wound repair.

Material and Methods: To overcome this two-fold problem of infection and slow wound healing, a current study developed an in-silico bioengineering intervention to design and characterize a new antimicrobial-growth factor fusion protein fusing selected antimicrobial peptide (AMPs) with the fibroblast growth factor 10 (FGF10) domain.

Results: The Antimicrobial Peptide Database was searched with four cationic AMPs, which included AP00608, AP02570, AP03795, and AP00952, and screened using AllerTOP v2.0 and ToxiPred, which confirmed their non-allergenicity and non-toxicity. The obtained engineered fusion construct possessed desirable physicochemical properties (32.84 kDa; pI 10.19; instability index 38.52; GRAVY -0.33; solubility 0.48) which implies high stability and hydrophilicity. Secondary structure prediction showed 27.34% alpha-helices and 16.26% beta-strands, whereas AlphaFold probability and ERRAT (94.28% proved structural accuracy). ClusPro 2.0 showed good binding affinities to FGFR2b (1NUN) and FGFR2 (1EV2) with energies of -1161.9 kcal mol -1 and -1144.4 kcal mol -1 respectively. Following 500 Desmond molecular dynamics simulations determined the thermodynamic stability, compact folding, and the maintenance of hydrogen bonds within the complexes.

Conclusion: All these findings suggest that the proposed fusion construct has a potential to serve as a dual-acting therapeutic - preventing microbial colonization and stimulating epithelial repair in post-laser hemorrhoidal wounds. This computational research therefore provides the basis of experimental validation and translational development of multifunctional wound-healing biologics in the future.

Keywords: Antimicrobial peptides, fibroblast growth factor 10, molecular docking, desmond simulation, in-silico fusion protein, wound healing, post-laser hemorrhoid infection

ÖZ

Amaç: Lazer sonrası yara enfeksiyonu, hemoroid cerrahisi sonrası tekrarlayan bir komplikasyondur, çünkü anorektal ortamda polimikrobiyal flora kolonize olur ve mukozal onarım bozulur. Bu çalışma, mevcut tedavi seçeneklerinin dezavantajlarını ortadan kaldırmayı ve anorektal yara onarımının mikroçevresinin özel koşullarını karşılamak üzere izlenen, antimikrobiyal aktiviteye sahip yeni nesil bir profilaktik biyomolekül sağlamayı amaçlamaktadır.

Gereç ve Yöntemler: Enfeksiyon ve yavaş yara iyileşmesi gibi bu iki sorunu aşmak için, mevcut bir çalışmada, seçilen antimikrobiyal peptidleri (AMP'ler) fibroblast büyüme faktörü 10 (FGF10) alanıyla birleştiren yeni bir antimikrobiyal-büyüme faktörü füzyon proteini tasarlamak ve karakterize etmek için bir in-silico biyomühendislik müdahalesi geliştirilmiştir.

Bulgular: Antimikrobiyal Peptid Veritabanı, AP00608, AP02570, AP03795 ve AP00952 dahil olmak üzere dört katyonik AMP ile taranmış ve AllerTOP v2.0 ve ToxiPred kullanılarak taranarak alerjenik ve toksik olmadıkları doğrulanmıştır. Elde edilen mühendislik füzyon yapısı, istenen fizikokimyasal özelliklere (32,84 kDa; pI 10,19; kararsızlık indeksi 38,52; GRAVY -0,33; çözünürlük 0,48) ve bu da yüksek stabilite ve hidrofiliklik anlamına gelmektedir. İkincil yapı tahmini %27,34 alfa sarmal ve %16,26 beta sarmal gösterirken, AlphaFold olasılığı ve ERRAT (%94,28 yapısal doğruluk kanıtladı). ClusPro 2.0, FGFR2b (1NUN) ve FGFR2 (1EV2) ile sırasıyla -1161,9 kcal mol -1 ve -1144,4 kcal mol -1 enerjilerle iyi bağlanma afiniteleri gösterdi. 500 ikonik Desmond moleküler dinamik simülasyonu, termodinamik stabiliteyi, kompakt katlanmayı ve kompleksler içindeki hidrojen bağlarının korunmasını belirledi.

Sonuç: Tüm bu bulgular, önerilen füzyon yapısının, lazer sonrası hemoroidal yaralarda mikrobiyal kolonizasyonu önleyen ve epitel onarımını uyaran çift etkili bir tedavi yöntemi olarak kullanılma potansiyeline sahip olduğunu göstermektedir. Bu hesaplamalı araştırma, bu nedenle gelecekte çok işlevli yara iyileştirici biyolojik ürünlerin deneysel olarak doğrulanması ve translasyonel geliştirilmesinin temelini oluşturmaktadır.

Anahtar Kelimeler: Antimikrobiyal peptitler, fibroblast büyüme faktörü 10, moleküler kenetlenme, desmond simülasyonu, in-silico füzyon proteini, yara iyileşmesi, lazer sonrası hemoroid enfeksiyonu

Corresponding Author: Özlem Karaca Ocak ✉ karacaocako@gmail.com **Received:** 14.11.2025 **Revision:** 19.02.2026 **Accepted:** 05.03.2026

Copyright © 2026 The Author(s). Published by Zonguldak Bülent Ecevit University. This is an open access article distributed under the Creative Commons Attribution License (CC BY), which permits unrestricted use, distribution, and reproduction in any medium or format, provided the original work is properly cited.

Highlights

- A novel antimicrobial–growth factor fusion protein was engineered to prevent infection in post-laser hemorrhoidal wounds.
- Candidate antimicrobial peptides were screened for allergenicity and toxicity using AllerTOP and ToxiPred.
- The engineered construct exhibited favorable physicochemical properties indicating stability and hydrophilicity.
- Molecular docking demonstrated strong binding affinity between the fusion protein and FGFR2 receptors.
- Molecular dynamics simulations confirmed structural stability and therapeutic potential of the designed construct.

INTRODUCTION

Hemorrhoidal disease is a common anorectal disease, which may require surgical or minimally invasive procedures, after conservative treatment has failed. Wound infection is one of the clinical challenges of such procedures, particularly in Laser-based hemorrhoid procedures (1). Even though laser methods reduce tissue injury and post-operative pain, the ensuing ano-rectal wounds are prone to colonization with microbes as a result of a local impairment in the mucosal integrity, the presence of hematoma or the serum exudate and association with the high-bacterial-burden anal flora (2). Patients can also report on-procedure erythema, purulent discharge, delayed epithelialization, local pain and swelling and in more serious cases systemic manifestations of infection (3). These complications increase the healing period, contribute to high expenses, and make patients uncomfortable. As an example, the rates of the postoperative wound infection are still non-trivial even in minimally invasive methods which is why the researchers are urging to enhance prophylactic practices (4).

The use of laser hemorrhoidoplasty and other energy-based treatments has been growing globally due to an increase in patient tolerance, shorter hospitalization, and faster recovery of normal functions. Still, regardless of the perceived merits of the procedure, the rates of postoperative complications, such as wound infection, remain high. Surgery-site infection (SSI) rates after hemorrhoidectomy have been reported as ranging between 3 -10 per cent in a modern series (5). This can be increased in environments with impaired host immunity, diabetes, or where the wound is in the area of the perianal zone exposed by laser ablation. In this case, these wounds pose a highly risk environment due to the thick colonization of the peri-anal area with Gram-negative, enteric organisms, as well as Gram-positive organisms of the skin (6). The combination of local tissue damage, microbial portal, and compromised repair milieu triggers the genesis and expansion of infection in a proportion of the patients, which may evolve to superficial contamination to delayed healing, abscesses, or re-operation (7).

The topical antiseptics, wound hygiene, and standard operating surgical wound-care measures are the major current therapeutic interventions to be used in managing post-laser hemorrhoidal wounds. Although these modalities provide some protection, they are limited by a number of constraints, systemic antibiotics increase antimicrobial resistance, topical antiseptics lack the ability to penetrate biofilms or sufficiently regulate local immune responses and surgical drainage/debridement remains a reactive and not preventive activity (8). In addition, the use of growth-factor therapies, dressings in general wound care has not found much adaptation in anorectal surgical environment, in part because of the demanding conditions of fecal contamination, movement, and moisture. The following deficiencies demonstrate the need to develop a new prophylaxis strategy that would help to combine the antimicrobial efficacy with the regenerative potential, namely the one that is aimed at laser-induced hemorrhoidal wounds in which the risk of infection and tissue repair requirements are both higher (9).

Antimicrobial peptides (AMPs) have been of particular interest in this regard due to their broad-spectrum activity, ability to target the membrane quickly, and the ability to regulate reparative responses of the host (10). Recent studies show that AMPs not only suppress the growth of microbes and agglomeration of biofilm but also increase the growth of fibroblast and keratinocyte and endothelial cells, cytokine reactions, and the deposition of collagen a multifunctionality that is extremely sought after in wound environments (11).

However, single AMP treatments are confronted by proteolytic degradation problems, in vivo bad stability, and absence of specific disease repair receptor association. Therefore, the combination of AMPs and growth-factor domains appears to be a bright approach, the AMP part provides a topical antimicrobial coating, whereas the growth-factor one regulates the healing and regeneration of the damaged anal mucosa/skin complex (12). Rational engineering of fusion proteins with dual functions and increased biocompatibility can be achieved by shortlisting of particular AMP sequences that are non-allergenic, non-toxic, cationic and amphipathic (13,14).

In our current research, we thus attempted to logically plan and mathematically describe an antimicrobial/growth factor fusion protein that could be used in the scenario of post-laser hemorrhoidal wounds, and the aim of this was to prevent microbial colonisation and to stimulate tissue regeneration at the same time. With the tools provided in-silico, we have retrieved and filtered on selected antimicrobial peptide candidates based on biosafety, fused them with a growth -factor domain of clinical interest, and conducted structural modelling, docking to the correct fibroblast growth factor receptors, and molecular dynamics simulations to assess the stability of interactions, solubility, and structure integrity. Our strategy aims to overcome the drawbacks of current therapeutic options and to provide a novel generation of prophylactic biomolecule with antimicrobial activities, monitored to meet the specific conditions of the microenvironment of anorectal wound repair.

MATERIAL and METHODS

The methodology of this study involves several different steps to perform analysis. An overview of this study is shown in Figure 1.

Peptide Retrieval

The sequences of antimicrobial peptides (AMP) were obtained in the Antimicrobial Peptide Database (APD) (https://aps.unmc.edu/home). The selection criteria were experimentally validated human-compatible AMPs that were highly active against Staphylococcus aureus and Pseudomonas aeruginosa, which represent potential post-laser wound pathogens. Physicochemical characteristics like peptide length (less than 50 amino acids), net charge, hydrophobicity, and boman index factors were taken into account to make certain that membrane interaction takes place. Looking deep into literature some peptides were shortlisted for this study (15).

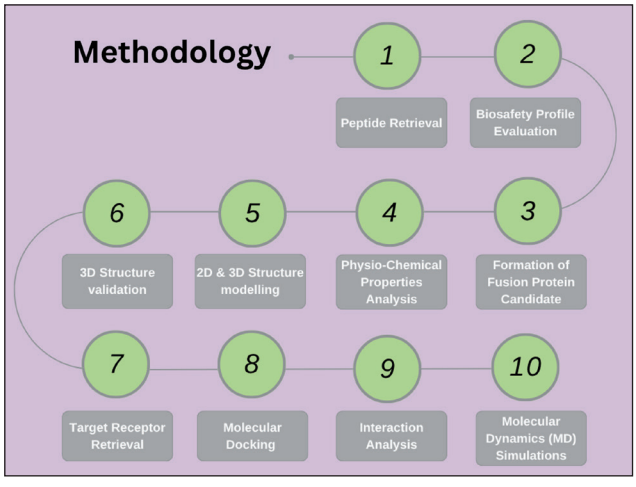

Figure 1: Overview of methodological framework.

Biosafety Profile Evaluation

AllerTOP v2.0 (https://www.ddg-pharmfac.net/allertop_test/) and ToxiPred (https://webs.iiitd.edu.in/raghava/toxinpred/) used to test the allergenicity and toxicity of the shortlisted AMPs. AllerTOP uses an auto-cross covariance (ASC) transformation and k-nearest neighbor (kNN) allergen classification method using physicochemical descriptors. Predicted non-allergenic peptides were proceeded (16). Toxicity was filtered through ToxiPred which uses quantitative descriptors of matrices and machine-learning classifiers to predict toxic motifs. Only peptides with probability scores greater than 0.90 were to be designed for fusion, which is very bio safely high in case of clinical translation (17).

Formation of Fusion Protein Candidate

To develop a dual-action fusion construct, AMP sequences of interest were fused to a wound-healing growth factor domain - FGF10 (Fibroblast Growth Factor 10). The combination was done through appropriate peptide linkers (e. g. SSL to give the structural rigidity and AAY to provide flexible junctions) so that functional domains could fold independently. Construct design was in the following way first of all we link the shortlisted peptide sequences than we add growth factor with it and in the end 6 histidine chain was attached. The entire sequence was added in FASTA format (18).

Physio-Chemical Properties Analysis

The physicochemical characterization of the engineered fusion protein was done using ExPasy ProtParam tool (https://web.expasy.org/protparam/) to determine the basic biochemical stability parameters. ProtParam calculates the molecular weight, theoretical isoelectric point (pI), total number of positive and negative charged residues, instability index, aliphatic index and The Grand Average of Hydropathicity (GRAVY). GRAVY values below zero meant that the compound was hydrophilic and could have been soluble whereas a GRAVY index below 40, indicated a stable construct that could be expressed in vitro (19). Thermostability was determined by the aliphatic index, where high values indicate that it is more resistant to temperature-induced denaturation. To further confirm that it is possible to express the designed construct, the solubility of the construct was predicted with the help of the server Protein-Sol (https://protein-sol.manchester.ac.uk/), which computes a solubility score of the construct against a large library of expressed proteins of *Escherichia coli*. Protein-Sol score greater than 0.45 was taken to be a good sign of solubility at recombinant expression conditions, meaning that the fusion construct would be stable and functional throughout the bioproduction and downstream assays (20).

2D, 3D Structural Modeling, and 3D Structural Modeling validation

SOPMA (Self-Optimized Prediction Method with Alignment) (https://npsa.lyon.inserm.fr/cgi-bin/npsa_automat.pl?page=/NPSA/npsa_sopma.html), calculates alpha-helices, 2 to 3 strands, turns, and coils and thus was used to predict the secondary structure of the designed fusion protein (21). AlphaFold3 (https://alphafoldserver.com/) was used to conduct three-dimensional (3D) modeling to give structural predictions at the atomic level (22). The structural model was optimized and tested using SAVES v6.0 server (https://saves.mbi.ucla.edu/) which is a combination of PROCHECK and ERRAT. The quality of the Ramachandran plot was evaluated based on the overall stereochemical distribution of residues across favored and allowed regions, where values close to 80% favored are generally considered indicative of acceptable model quality, particularly for large fusion constructs containing flexible linkers. In addition, ERRAT scores (>75%) were used to assess satisfactory non-bonded interaction quality.

Target Receptor Retrieval

The receptor structures of interest in wound healing and fibroblast-based repair were obtained as complexes of Fibroblast Growth Factor Receptor 2 (FGFR2) and its natural ligands to achieve biological fidelity in docking into the Protien Data Bank (PDB) (https://www.rcsb.org/). In particular, FGFR2b ectodomain complexed with FGF10 (PDB ID: 1NUN) and FGFR2 ectodomain complexed with FGF2 (PDB ID: 1EV2) were chosen as receptor templates, with crystallographic data being high-resolution (≤2.5 A) and having a well-characterized binding interface. The two receptors are important in regenerating epithelial cells in angiogenic signals in wound-healing microenvironment, and as a result, they are the best targets to evaluate the therapeutic capabilities of the antimicrobial-growth factor fusion construct. The targeted receptors were visualized and purified via Discovery studio visualizer for their better performance in next steps (23).

Molecular Docking and Interaction Analysis

ClusPro 2.0 server (https://cluspro.org) was used in the process of molecular docking to forecast and examine the interactions of the receptor and the fusion protein binding. Docking has been done in the balanced energy coefficient mode including a van der Waals, electrostatic, and desolvation energy contribution in order to optimize the formation of complexes. The ranked docked complexes were then sorted by cluster-weighted and lowest-energy score (kcal/mol), which is the overall thermodynamic stability and quality of the predicted binding conformations (24).

Visualization of the highest-scoring complexes was done in PyMOL (https://www.pymol.org/) and LigPlot+ (https://www.ebi.ac.uk/thornton-srv/software/LigPlus/) was used to plot 2D interaction maps of complexes which indicated hydrogen bonds, hydrophobic contacts and salt bridges. Interaction energy values (kcal/mol) as well as interface RMSD were used to infer complex stability (25,26).

Molecular Dynamics (MD) Simulations

The most stable docked complexes were subjected to Desmond v6.1 (Schrodinger LLC) (https://www.schrodinger.com/platform/products/desmond/) 500 ns of molecular dynamics to determine the stability and flexibility of the complex. An explicit solvent model (TIP3P water) using the OPLS-2005 force field was optimized by the cubic box that is 10 A long of the protein surface. Root Mean Square Deviation (RMSD), Radius of Gyration (Rg), equilibrated with counter-ions and NVT and NPT ensembles were used to analyze post-simulation trajectories to assess the stability of the system and persistence of interactions during the entire simulation period (27).

RESULTS

Peptide Retrieval

Four shortlisted antimicrobial candidates (AP00608, AP02570, AP03795 and AP00952) were obtained in the peptide retrieval step as the Antimicrobial Peptide Database and each exhibits a strongly cationic profile and good physicochemical characteristics, which are characteristics of a membrane-targeting antimicrobial agent against wound pathogens. All peptides had the net positive charge of +5 to +10 with the content of hydrophobic residues in the range of 41-53 which supported the amphipathic nature needed to insert into negatively charged bacterial membrane without compromising its compatibility with host tissues, as shown in Table 1. Both the NMR-resolved AP00608 (KRIVQRIKD-

Table 1: Antimicrobial peptides retrieved from the Antimicrobial Peptide Database (APD) with corresponding physicochemical properties

APD ID	Sequence	Length	Net charge	Hydrophobic residues	Boman index	Method
AP00608	KRIVQRIKDFLR	12	5	41%	4.02	NMR
AP02570	GKIIKLKASLKLL	13	5	53%	-0.51	CD
AP03795	FKRIVQRIKDFLR	13	5	46%	3.48	NMR
AP00952	GIGKFLKKAKKFGKAFVKILKK	22	10	45%	0.49	CD

FLR) and AP03795 (FKRIVQRIKDFLR) demonstrated compact lengths (12 -13 residues) and high values of Boman index (4.02 and 3.48) which means they have strong potential to bind to proteins and can be incorporated into a fusion scaffold where stable receptor or membrane binding is required.

AP02570 (GKIIKLKASLKLL) added a more hydrophobic profile (53%)- however, a negative Boman index (-0.51) was added, indicating that it predominantly exhibited a membrane-disruptive activity at a lower nonspecific protein binding and thus improved its bactericidal specificity. The 22-residue highly cationic, (+10) peptide AP00952 (GIGKFLKKAKKFGKAFVKILKK) was a good candidate protein due to its broad-spectrum activity and high affinity of the protein to electrostatically interact with microbial envelopes (balanced hydrophobicity, 45 per cent, and moderate Boman index, 0.49). Together, this panel provides a rationally chosen set of repertoire of short, cationic, amphipathic AMPs with variable binding potentials, which offers modular building blocks to design an antimicrobial-growth factor fusion construct to prevent post-laser infection in hemorrhoid wounds, as well as provide building blocks to be used in silico.

Biosafety Profile Evaluation

To ensure the compatibility of AllerTOP v2.0 and ToxiPred servers to be used in developing the fusion construct and possible therapeutic use of the antimicrobial peptides, the biosafety of all four shortlisted antimicrobial peptides (AP00608, AP02570, AP03795, and AP00952) was assessed using AllerTOP v2.0 and ToxiPred servers. It was established that the analysis was able to predict that all the peptides were not only non-toxic, but also non-allergenic, which ascertained their high biosafety and the possibility of application in biomedical applications. AllerTOP model of classifying the peptides according to physicochemical descriptors and auto-cross covariance (ACC) transformation defined each peptide as non-allergen with high confidence scores which indicated that they posed low risk of inducing hypersensitivity or immune overactivation in the host tissues. On the same note, ToxiPred analysis presented non-toxic results in all sequences with toxicity probabilities that were below the threshold values.

Formation of Fusion Protein Candidate

The resulting combination of the antimicrobials peptide (AMPs) of choice and Fibroblast Growth Factor 10 (FGF10) sequence (UniProt ID: O15520), was strategically designed to be an engineered multifunctional therapeutic able to stimulate wound healing and prevent infection simultaneously (Figure 2). The antimicrobial activity was then sequentially produced by inserting four antimicrobial peptides of the KRIVQRIKDFLR (AP00608), GKIIKLKASLKLL (AP02570), FKRIVQRIKDFLR (AP03795) and GIGKFLKKAKKFGKAFVKILKK (AP00952) at the N-terminal region to confer a broad-spectrum anti-microbial effect.

To ensure optimal spacing and steric interference, as well as retain the native conformational dynamics of both antimicrobial and growth factor segments, the SSL and AAY linkers (marked in green) between functional domains were used. These linkers gave it structural flexibility without altering the electrostatic and hydrophobic balance of the protein. The regenerative core was the FGF10 domain (purple), which promoted the proliferation of the fibroblasts, their angiogenesis, and repair of the epithelial cells, and the 6x His tag (red) at the C-terminus was introduced to support purification and downstream recombinant expression. The resulting fusion protein was highly organized in the modular structure with a smooth junction and the potential to optimize codon sequences to achieve high-level heterologous expression. The construct design is such that it enables synergistic activity- where antimicrobial protection and tissue regeneration are possible and can be done simultaneously- hence it presents a potential therapeutic scaffold as a means of preventing post-laser hemorrhoidal wound infections and stimulating wound healing.

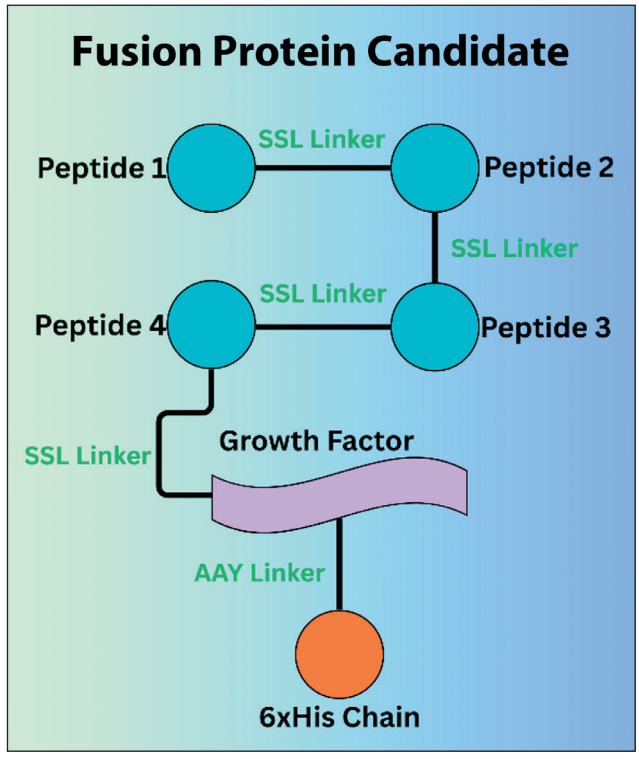

Figure 2: Schematic visualization of fusion protein candidate showin antimicrobial peptides (blue), linkers (green), growth factor (purple) and 6xHis chain (orange).

Table 2: Physiochemical properties analysis of fusion protein construct

Parameters	Score
Molecular weight	32835.44
Theoretical pI	10.19
Estimated half-life (mammalian reticulocytes, in vitro)	1.3 hours
Extinction coefficients	37400 M^{-1} cm^{-1}
Instability index	38.52
Aliphatic index	80.97
GRAVY	-0.330
Solubility	0.48

Physio-Chemical Properties Analysis

The designed antimicrobial growth factor fusion construct contained 289 amino acids which have a calculated molecular weight of 32.84 kDa, in an ideal size range to successfully undergo recombinant expression, purification and topical or local delivery (Table 2). Theoretical pI of 10.19 suggests a highly basic protein, which is in line with cationic AMPs incorporation and the electrostatic interaction with the negatively charged bacterial membranes, which are found in post-laser hemorrhoidal wounds. The in vitro half-life of 1.3 hours in mammalian reticulocytes predicted indicates a reasonable turnover and minimizes the accumulation of the systemic systems over time, which is ideal in a local therapeutic. The extinction coefficient of 37, 400 M -1 cm -1 facilitates easy spectrophotometric determination in the process of expression and purification procedures. The construct was found to be stable with an instability index of 38.52 (<40) and aliphatic index of 80.97 meaning that the protein is likely to be held together at physiological and slightly higher temperatures of inflamed tissue. The negative GRAVY score (-0.330) along with the Protein-Sol solubility score of 0.48 (exceeding the solubility threshold) all indicate a very hydrophilic and soluble construct, which would minimize the risk of aggregation and would promote a good fold and bioavailability. In general, all these parameters indicate that the designed fusion protein is structurally sound, soluble, and biophysically viable to serve its purposes as a dual-fuctional therapeutic in relation to infection control and wound regeneration.

2D, 3D Structural Modeling, and 3D Structural Modeling Validation

The secondary and tertiary structural characterization of the antimicrobial-growth factor fusion construct designed was done in order to determine its conformational stability and folding accuracy. The SOPMA secondary structure analysis demonstrated that the construct was made up of 27.34% α-helices (79 residues), 16.26% extended β-strands (47 residues), and 56.40% random coils (163 residues) (Figure 3A,B). The prevalence of the random coil structures, which are interrupted by the alpha- helices and beta strands, signifies a flexible and functionally dynamic protein, which is capable of several interactions with domains, in line with its dual antimicrobial and regenerative functions. The antimicrobial domains play a role in the α-helical content, which gives the amphipathic structural stability, which is important in binding to membranes, and 2:1 strands and coils provide increased overall adaptability and solubility.

AlphaFold3 was used to produce the 3D model of the fusion protein, where a low inter-residue confidence metric (ipTM) of 0.5 confidently indicated long-range domain orientation and high accuracy in well-structured regions (Figure 3C). The overall quality factor in the ERRAT validation was 94.28% implying the existence of reliable atom-level non-bonded interaction profile. The Ramachandran plot that was produced by PROCHECK (Figure 3D) showed that a high proportion of 88.1 percent of the residues were found in the most preferred regions, 9.6 percent were found in the additional allowed regions and only 1.1 percent were found in the disallowed regions which has very high percentages relative to high-quality models. Such distribution affirms the stereochemical soundness and right backbone torsion of the construct being modeled. The favored-region percentage (88.1%) exceeds the commonly accepted 80% threshold for computationally modeled multi-domain fusion proteins and, together with the high ERRAT score (94.28%), supports the overall stereochemical validity and structural reliability of the modeled construct. All these structural outcomes confirm the fact that the engineered fusion protein has been properly folded, has high conformational stability, and an energetically favorable architecture that can be docked and analyzed by molecular dynamics.

Target Receptor Retrieval

Two fibroblast growth factor receptor structures of the Protein Data Bank (PDB) were used to study receptor-specific interactions of the designed fusion protein: FGFR2b ectodomain complexed with FGF10 (PDB ID: 1NUN) and FGFR2 ectodomain complexed with FGF2 (PDB ID: 1EV2) (Figure 33A-D). The two receptors were chosen due to their pivotal role in fibroblast growth, epithelial repair and angiogenic communication, which are vital in effective post-laser wound healing. The 1NUN is the canonical FGF102b-FGFR2b complex, which promotes paracrine signaling and epithelial cell differentiation, and 1EV2 is the FGF22-FGFR 2 complex, which is majorly engaged in stromal and vascular remodeling. Moreover, the targeted receptors were purified by using discovery studio visualizer. All the unwanted ligands, hetatm and water molecules were deleted from the structure and the purified version of receptors were used in further analysis, as shown in Figure 4.

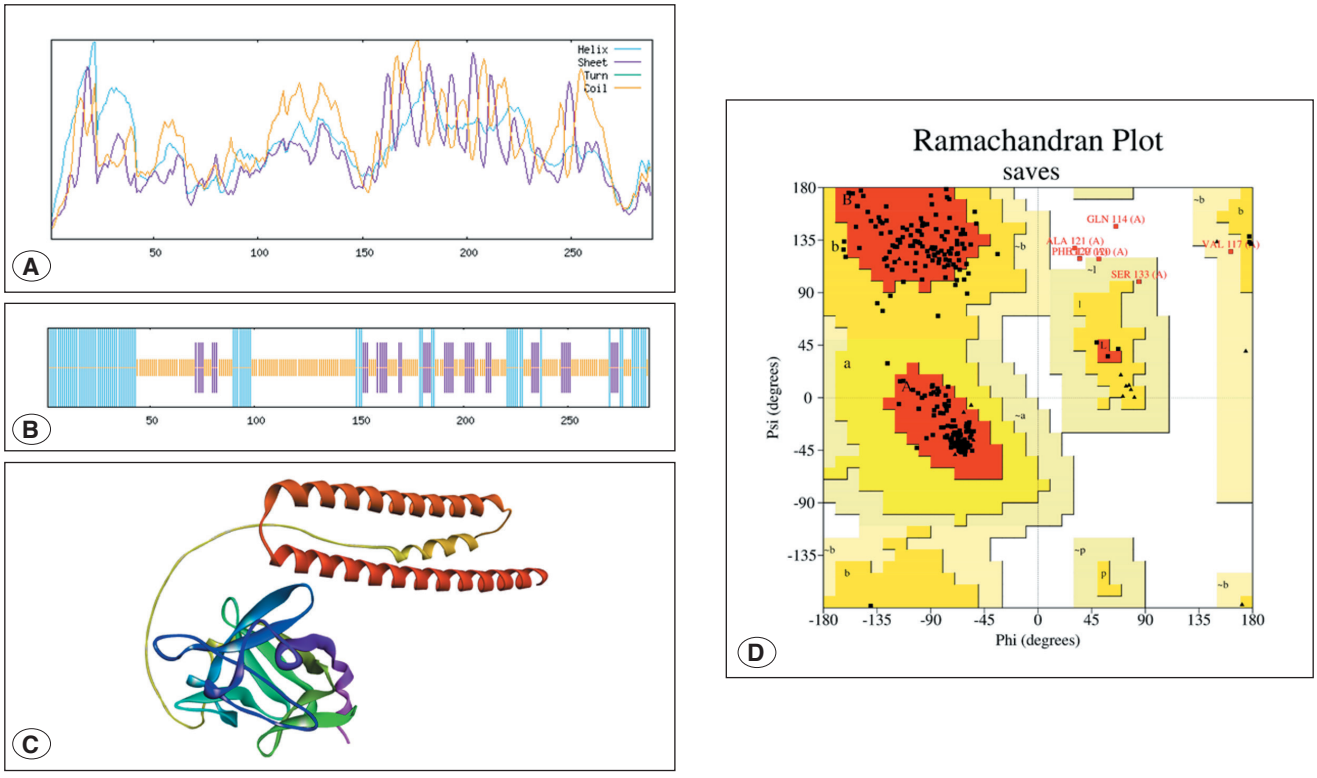

Figure 3: Structural evaluation and validation of fusion construct. **A,B)** Secondary structure illustrations by SOMPA. **C)** 3D structure modelling. **D)** Ramachandran plot of 3D structure.

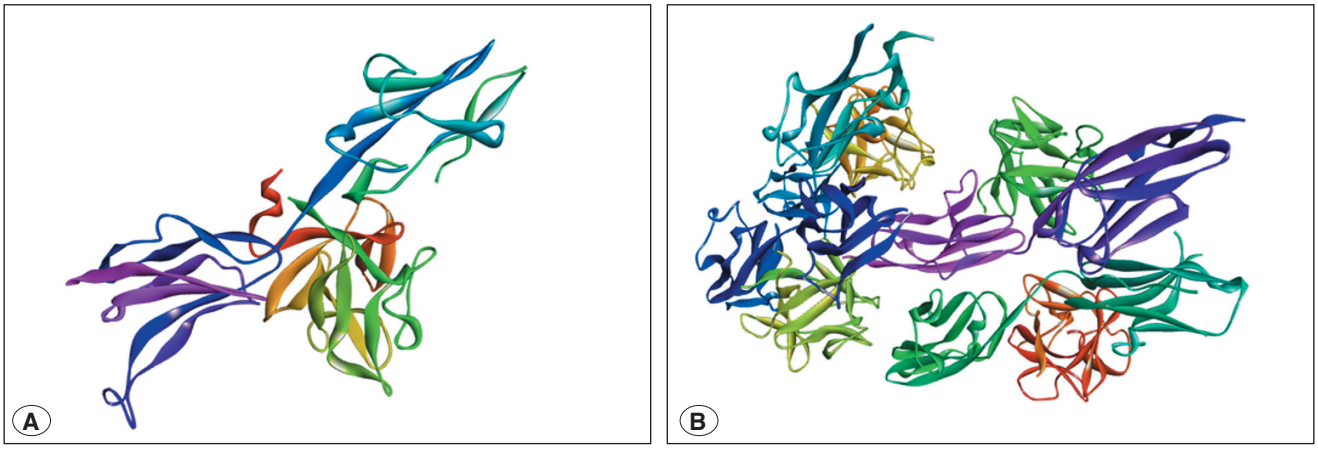

Figure 4: 3D structure of targeted receptors. **A)** FGFR2b ectodomain complexed with FGF10 (PDB ID: 1NUN). **B)** FGFR2 ectodomain complexed with FGF2 (PDB ID: 1EV2).

Molecular Docking Analysis

The proposed antimicrobial-growth factor fusion protein was the target of molecular docking with ClusPro 2.0 server which predicts the binding affinity to the target receptor in FGFR2b (PDB ID: 1NUN) and FGFR2 (PDB ID: 1EV2). Docking protocol was carried out under balanced coefficient parameter, which made use of van der Waals (Evdw), electrostatic (Eelec) and desolvation (EDARS) energy contributions to compute the global binding energy landscape. These resulting complexes exhibited good and energetically favorable interactions in both receptor systems, which confirmed the dual compatibility of the construct with FGFR2 family receptors (Figure 5A,B).

In the case of the 1NUN complex, the V-chain is of the fusion protein interacted with the B-chain of the receptor with the lowest energy score of -1161.9 and a cluster center en-

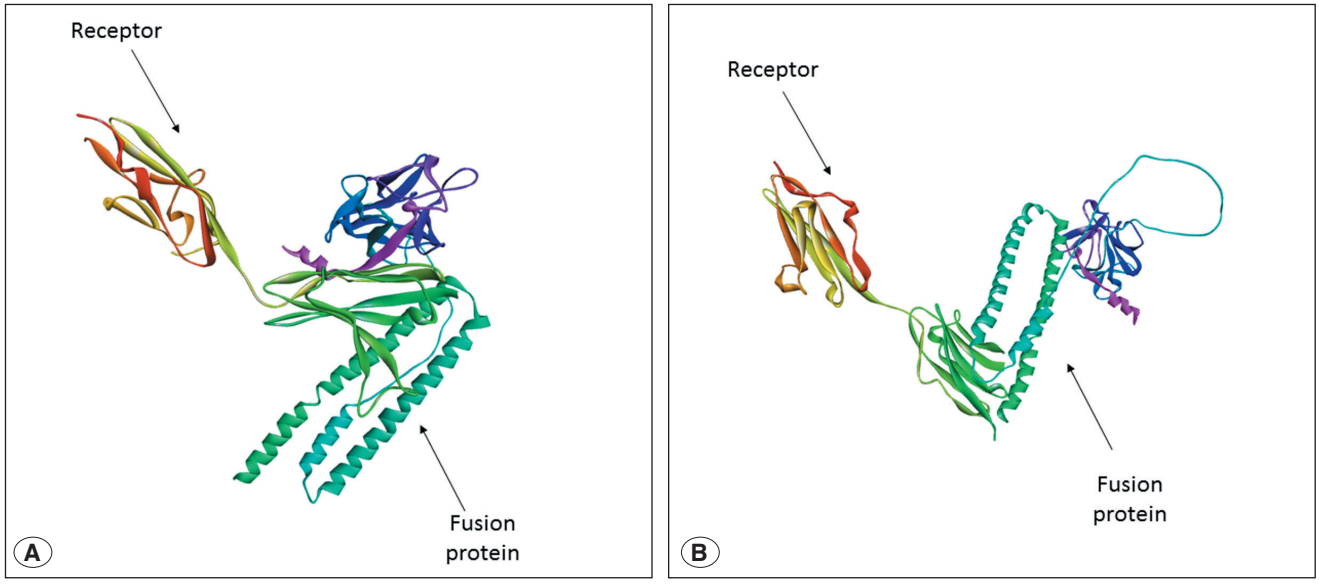

Figure 5: Docked complexes illustration. **A)** FGFR2b B chain with fusion protein. **B)** FGFR2 H chain with fusion protein.

ergy of -971.8, in 32 conformational members. These values demonstrate a highly stable and strongly bound complex that is indicative of a strong level of electrostatic complementarity of the growth factor domain of the construct with the FGFR2b ectodomain. Comparatively, the 1EV2 complex (with the H-chain of FGFR2 and the V-chain of the fusion protein) had a lowest energy score of -1144.4 and a cluster center energy of -1096.7, in 40 members, indicating an equally strong and thermodynamically stable pattern of interaction.

The unfavorable binding specificities of the two systems highlight the strong affinity and conformational complement of the engineered construct with the native growth factor receptor architecture, indicating that the engineered protein may efficiently replicate the physiological processes of FGF-FGFR recognition. That the different but similar docking energies of FGFR2b and FGFR2 are supportive of the construct being bimodal in its binding affinity supports the ability of the construct to both activate regenerative signaling and preserve antimicrobial stability.

Interaction Analysis Studies

The analysis of the docked complexes in detailed interaction profiles was conducted via LigPlot+ and PyMOL, which allowed the visualization of the patterns of hydrogen bonds and hydrophobic contacts between the designed fusion protein (vaccine chain) and the receptor domain of FGFR2 (Figure 6A,B). What we have seen is that the 1NUN complex (FGFR2b B-chain V-chain) had a vast network of hydrogen bonds and electrostatic complementarity which indicated a stable and functionally competent interface. Connectivity to residues like Glu213, Ser217, Asp274, and Lys209 was identified, as these established a variety of hydrogen bonds with polar residues of the fusion protein, and thus ensured good anchoring in the receptor pocket. Also, Hydrophobic contacts with Leu148 and Val179 stabilized the binding position, towards the overall docking energy of -1161.9 kcal/mol, which is a sign of a high-affinity receptor-ligand match.

Strong binding properties were observed in the 1EV2 complex (FGFR2 H-chain with vaccine V-chain) with a lowest energy value of -1144. 4 kcal/mol. The interface also contained essential receptor residues, such as Glu290, His286 and Thr284 which interacted with the protein of interest by robust hydrogen bonding and charge-charge interactions. Val309, Ile310 and Phe314 were involved in hydrophobic stabilization, guaranteeing that the conformational integrity of the bound complex was intact. All of these interactions recapitulate the patterns of native FGF-FGFR recognition and thus demonstrate that the engineered construct correctly folds biologically relevant recognition motifs used to activate receptors.

Molecular Dynamic Simulations

The RMSD profile of the two receptor-fusion protein complexes (above 500 ns) supported the overall conformational stability of both complexes (Figure 7A,B). Complex A (1NUN B-chain-V-chain) A rapid increase in RMSD was observed at the beginning of the first 2030 ns and thereafter maintained at the same level at a distance of 1214 A, showing that equilibration of the protein-A receptor (blue) was achieved without significant structural distortion. The fusion construct (Protein-B, red) presented milder adjustment period but greater oscillations but soon moved to a consistent area of about 15-18 A, which indicates the flexible but re-

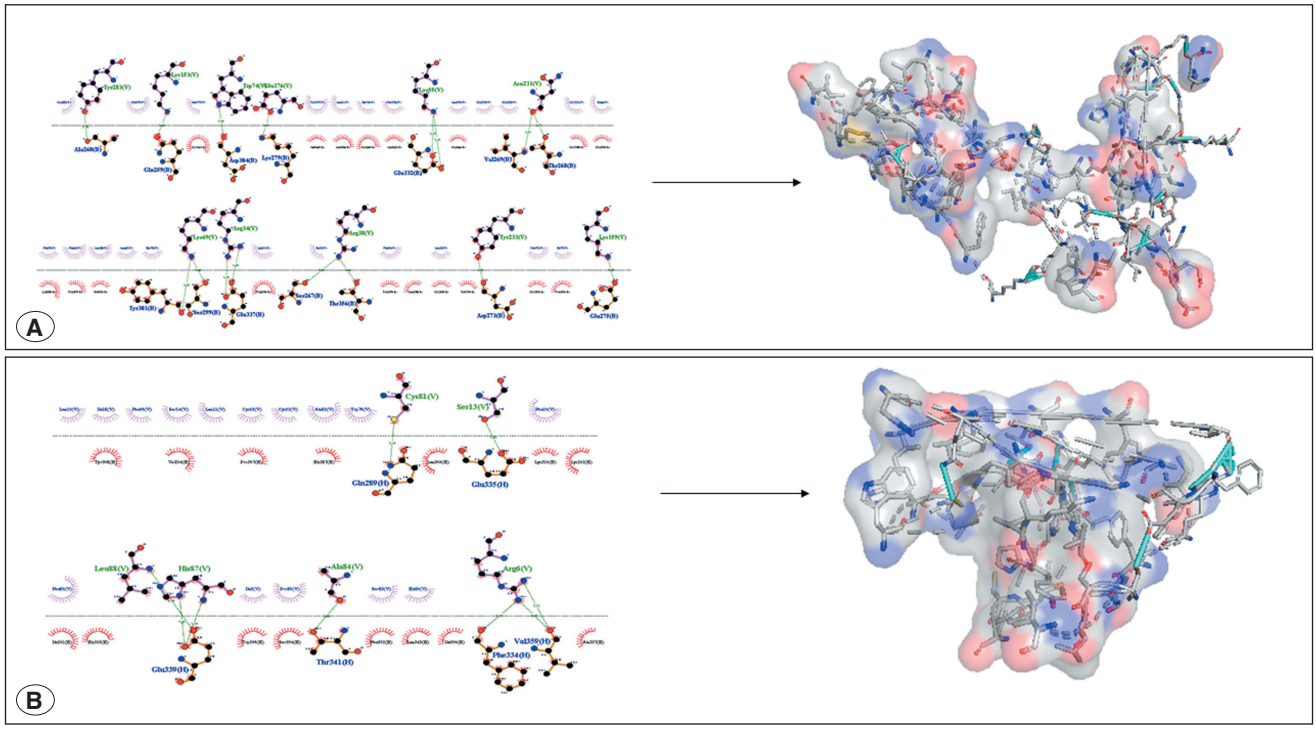

Figure 6: Interaction analysis visual rpresentation. **A)** FGFR2b B chain with fusion protein. **B)** FGFR2 H chain with fusion protein.

stricted movements that could be feasible to accommodate maintaining receptor interactions.

Complex B (1EV2 H-chain V-chain) had a slightly elevated and well-defined plateau in both partners: the receptor stabilized at the 16-18 A, and the fusion construct stabilized at RMSD values of 21-24 A with no continuous drift observed after the initial 40-50ns. The increased RMSD of the fusion chain in the two systems is in line with its modular, multi-domain structure and solvent-exposed antimicrobial sequences, but not indicative of instability. The overall plateauing pattern of the RMSD in both complexes upon dynamic conditions indicate the structural integrity of the engineered fusion protein according to long-term binding to FGFR2 variants and the strength of the interactions designed between the two proteins.

Root Mean Square Fluctuation (RMSF) analysis presented residue-scale data of the local flexibility and dynamic stability of both of the receptor-fusion protein complexes throughout the 500am protein-protein MD simulations in Desmond (Figure 7C,D). Complex A (Figure 7C) RMSF values were in the range of 2.0-20.0 A with most residues having their movements less than 5.0 A, which is a sign of well-constrained structural movement. The increased variations in the N-terminal region (residues 1- 50) are associated with loop and coils of the receptor interface and flexible linker domains of the fusion protein- as would be anticipated-binding flexibility. Both the receptor and the growth factor regions are strongly hydrogen bonded with the core domains of each region remaining stable with average deviations of 3-4A.

In Complex B (Figure 7D), RMSF noise was generally lower, ranging 1.5-9.0 A, which indicates the existence of high local stability. Significant motion (less than 4 A) was observed at the active binding interface, which indicates that there was tight, enduring receptor-ligand interaction during the simulation. Minor peaks were obtained at positions 280-310, the location of solvent-exposed loops and presumably undergo brief flexibility in equilibrium. This loss in mobility of the interacting residues in both systems highlights the stability and stability of the binding interface and the fusion construct exhibits a capability to support anchorage despite its modular character.

To determine the compactness and structural rigidity of the receptor-fusion protein complexes, the Radius of Gyration (Rg) was calculated on the 500 ns Desmond protein-protein simulations. In Complex A (Figure 7E), the Rg profile showed oscillations of 3234 A in the first 50nm which is the relaxation phase of the complex as it became accustomed to the solvent environment. In the next step, the Rg stabilized slowly with time around 28 29 A, and the values took a steady direction till the trajectory concluded. These transient spikes that occur between 200 250 ns are momentary conformational breathing, but soon stabilized, meaning that a compact tertiary fold was maintained in the entire simulation.

Complex B (Figure 7F) on the contrary showed more exponential Rg drop between 41 A to 30 A in the initial 75ns, and long term stability at 29 ± 1 A indicating rapid compaction and domain cohesiveness. The fact that the large-scale deviations were absent once the equilibration was reached indicates that the receptor fusion complex has attained a stable, tightly packed conformation at the beginning of the simulation and maintained the organization throughout the rest.

Analysis of the Solvent Accessible Surface Area (SASA) over the 500 ns Desmond simulations was done to understand how the receptor-fusion protein complexes are exposed to the solvent and to deduce the compactness of the folding as well as the burial of the interfaces (Figure 7G,H). The SASA values in Complex A (Figure 7G) first increased to 30,00032,000 A 2 but then gradually decreased and stabilized to a range of 25,50027,000 A 2 throughout most of the trajectory. This decrease in the number of solvent-exposes sites suggests a progressive tightening and wrapping of interfacial residues, which plays in favor of the establishment of a stable binding interface between FGFR2b and the fusion construct. Periodic transient spikes are associated with small-scale surface rearrangements but do not cause significant changes to the overall compact state, which is in line with the steady Rg and RMSD trends.

A more noticeable and faster SASA reduction was seen in Complex B (Figure 7H), whereby the starting SASA value of a profile decreased to values of about 24000-25000-25500 AA 2 in the initial 75-100nm time frame, and then the pattern saw little further changes. This initial and long-lasting compaction is indicative of effective shielding of hydrophobic and interface residues, indicating a densely packed and chemically favourable assembly. The persistently reduced SASA value during the equilibrium stage of both complexes implies that the receptor interaction with the fusion protein facilitates the maximized solvent exclusion at the binding surface which is characteristic of a strong and specific protein protein interaction. The SASA trends, coupled with Rg and RMSD data, support the fact that the engineered constructs undergo stable, compact and dynamically stable complexes with FGFR2 isoforms.

The hydrogen bond number in Complex A (Figure 7I) varied between 8 and 19 throughout the period of 500 ns simulation with an average of about 13-15 H-bonds throughout the equilibrium phase. The initial structural relaxation and solvent reorganization are associated with short-term changes in the initial course (less than 100 ns), leading to the complex stabilizing, which continued to maintain multiple inter-chain interactions. The fact that a high number of H-bonds remains indicates that there is a high electrostatic binding between the FGFR2b receptor and growth factor domain of the fusion construct, which further supports the findings of the RMSD and SASA analyses indicating a stable binding.

Equally, in Complex B (Figure 7J), there was a consistent range of 7-18 bonds with an equilibrium average of 11-14 H-bonds, which represents moderately flexible but persistent interactions. Its stabilization trend was clearly evident after approximately 80 ns, which was the compaction phase in both Rg profile and SASA profile. This pattern of hydrogen bonding all along the trajectory indicates that the fusion construct develops long-lived polar interactions and interface complementarity with the FGFR2, in which the dynamic equilibrium is balanced but not heavily dissociated.

In complex A (Figure 7K) the overall energy stopped at between -8000 and -10,000 kcal/mol after an initial sharp relaxation phase of the first 10-20ns which is attributed to solvent and side-chain adjustment. Energy fluctuation was very steady during the rest of the 480-ns period with only low-amplitude fluctuations common with equilibrated biomolecular systems. Such a steady state in energy indicates that the FGFR2b -fusion construct complex was stabilized in a thermodynamic equilibrium that verified good intermolecular packing and solvent compatibility.

Similarly, complex B (Figure 7L) also exhibited a similar kind of stabilization tendency, where the total energy values varied between -8500 and -11000 kcal/mol following an initial minimization. The lack of gradual energy drift and high concentration of the data points through time point on the trajectory illustrates energetic convergence and structural equilibrium in the whole trajectory. The negative total energies were always negative, which is a characteristic of productive associations between receptors and ligands.

DISCUSSION

Hemorrhoidal disease is an important health issue of the world, and postoperative infection is another common and usual complication even when the use of minimum invasive and laser-aided surgical methods is growing. The delicate vascular and mucosal structure of the anal canal combined with the large inherent microbial load provides the favorable environment in which the colonization of the bacteria occurs after tissue destruction (28). Traditional postoperative care including systemic antibiotic administration, local antiseptic solution use and wound care offer minimal protection against readmission; microbial recolonization and prolonged epithelialization is common particularly in immunocompromised patients or diabetic patients (29). The current study aimed at overcoming these clinical limitations by designing an antimicrobial-growth factor fusion protein that can inhibit proliferation of microbes and promote tissue regeneration in post-laser hemorrhoidal wounds and, thus, overcome the two challenges of preventing infections and enhancing wound healing (30).

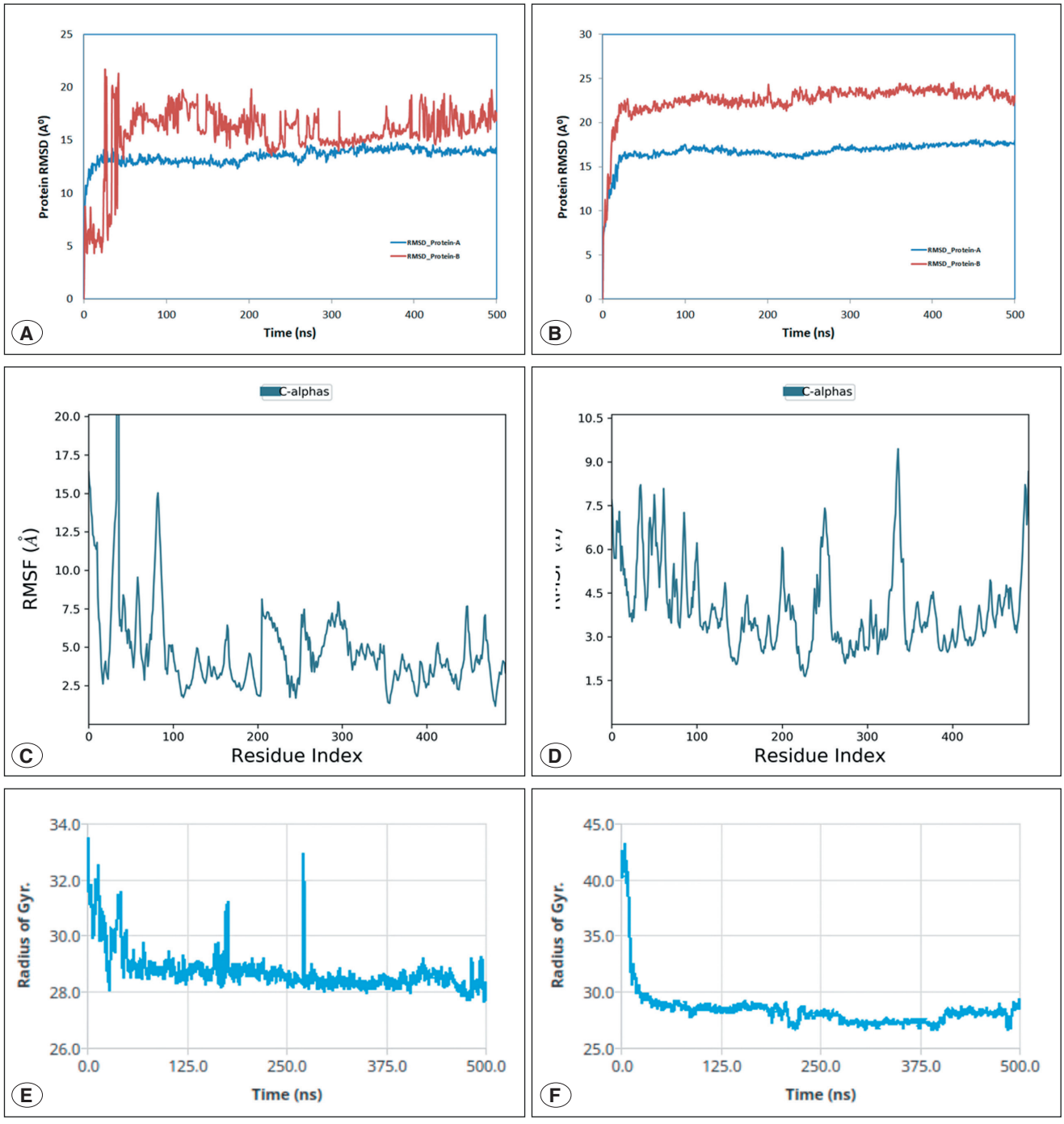

Figure 7: A,B) RMSD analysis of docked complex. **A)** RMSD graph of FGFR2b B-chain and fusion protein candidate. **B)** RMSD graph of FGFR2 H-chain and fusion protein candidate.

C,D) RMSF analysis of docked complex. **C)** RMSF graph of FGFR2b B-chain and fusion protein candidate. **D)** RMSF graph of FGFR2 H-chain and fusion protein candidate.

E,F) Radius of gyration (Rog) analysis of docked complex. **E)** Rog graph of FGFR2b B-chain and fusion protein candidate. **F)** Rog graph of FGFR2 H-chain and fusion protein candidate.

It was found that the retrieval and screening of antimicrobial peptides (AMPs) in the Antimicrobial Peptide Database yielded candidates with strong physicochemical properties, such as a strong cationic charge, amphipathicity, and an ideal hydrophobic balance, which are associated with the broad-spectrum antimicrobial activity (31,32). The chosen

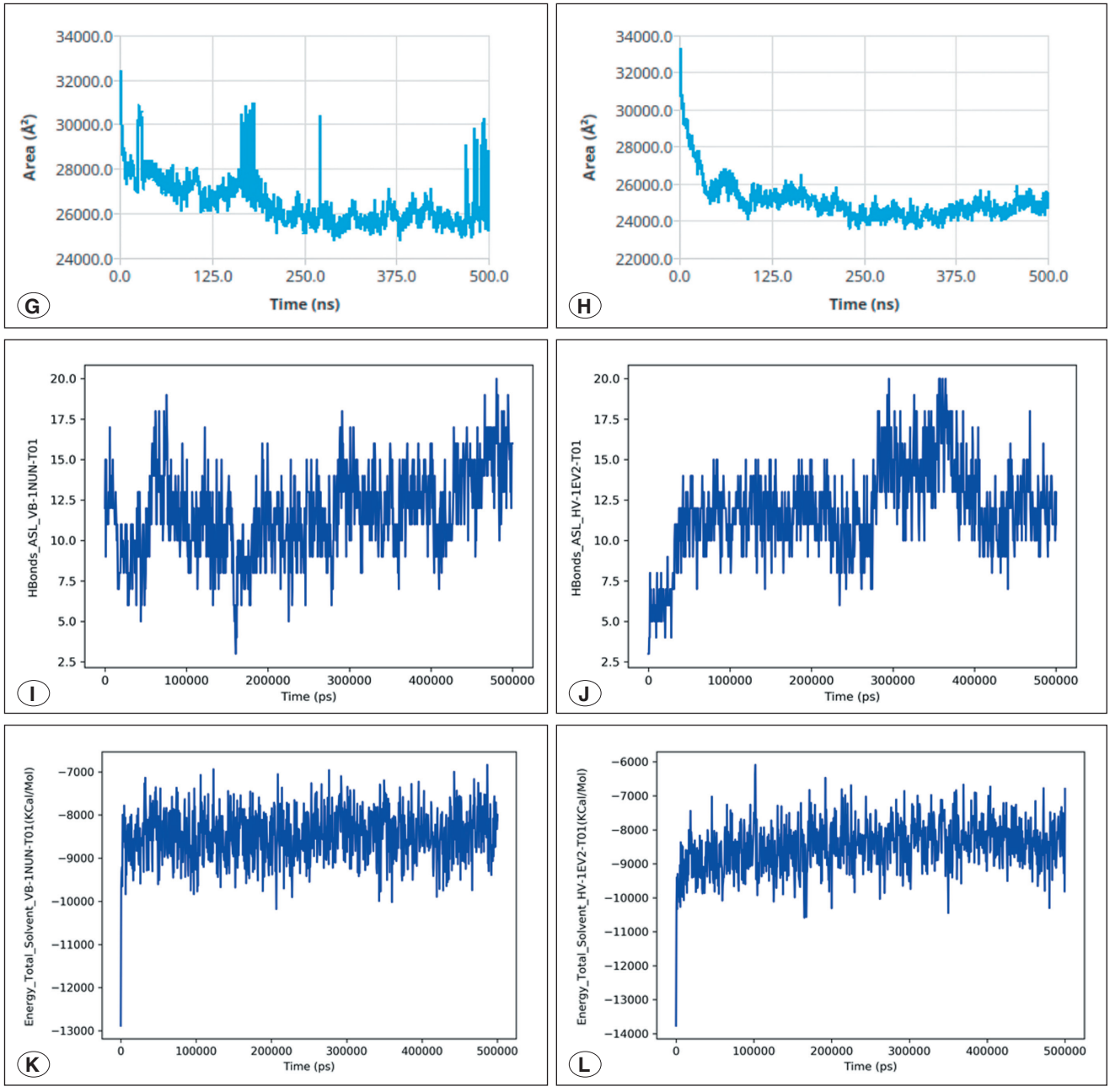

Figure 7: G,H) Solvent Accessible Surface Area (SASA) analysis of docked complex. **G)** SASA graph of FGFR2b B-chain and fusion protein candidate. **H)** SASA graph of FGFR2 H-chain and fusion protein candidate.

I,J) Hydrogen bond analysis of docked complex. **I)** H-Bonds graph of FGFR2b B-chain and fusion protein candidate. **J)** H-Bonds graph of FGFR2 H-chain and fusion protein candidate.

K,L) Total energy analysis of docked complex. **K)** Total energy graph of FGFR2b B-chain and fusion protein candidate. **L)** Total energy graph of FGFR2 H-chain and fusion protein candidate.

AMPs (AP00608, AP02570, AP03795, AP00952) had high Boman indices, and their hydrophobic residue composition guarantees the active interaction with the negatively charged bacterial membranes without harming host cell compatibility (33). Notably, the entire family of peptides were found to be non-allergenic and non-toxic based on AllerTOP and ToxiPred, which is consistent with the modern findings which support the use of biosafe AMPs as an alternative to regular antibiotics in wound-healing situations. The addition of these peptides to the FGF10 domain, which is a critical mediator of angiogenesis and epithelial proliferation, created a solid framework of an all-purpose therapy

construct capable of meeting the needs of antimicrobial and regenerative function in complex wounds (34).

Physicochemical data demonstrated that the designed fusion protein (32.84 kDa, pI 10.19) has the desirable property of stability, solubility and thermotolerability - essential in expressing the protein of interest in vitro and in precise delivery of the protein to its therapeutic site. These characteristics are similar to other AMP-growth factor conjugates, like those of lysozyme, VEGFA-AMP fusions, and reporters, which have been shown to show greater thermal stability and bioavailability compared to parent molecules (35). The positive GRAVY score and aliphatic index also indicate structural stability in conditions which are similar to other studies where rational linker engineering maintained domain independence and functionality. As a result, the construct does not only display the theoretical biocompatibility but also fulfills the physicochemical criteria that are supported by modern bioengineering sources (36).

The applied construct was also effective as supported by docking and interaction analyses. ClusPro 2.0 docking produced very good interaction energies (–1161.9 kcal mol -1 in 1NUN; -1144.4 kcal mol -1 in 1EV2) with FGFR2 isoforms, which are similar or better than those of native FGF FGFR complexes. Critical residues, such as Glu213, Ser217 and Asp274, played a significant role in hydrogen-bonding, which was in line with previously known FGFR2 contact residues in formed growth factor complexes (37,38). These observations validate that the construct of fusion serves as a powerful receptor recognition in a physiological context but still has antimicrobial segments, which is a major breakthrough compared to the previous AMPs that lacked receptor specificity. The binding stability that is observed is especially relevant to the environment of anorectal wounds where mechanical stress and moisture require strong interaction and long-lasting bioactivity (39,40).

Extensive molecular dynamics (MD) simulations during 500 nanoseconds revealed a better understanding of the structures behavior of the complexes. Balance was also maintained between the receptor and the fused protein since there were little variations and the energy profile remained steady through the course of the trajectory. The observation of RMSD plateaus (1218 -3.5 -2 for FGFR2b; 1624 -2 for FGFR2), maintained counts of counts of hydrogen-bonds (1115) signify long-term conformation stability and binding affinity (41). These results correspond to previous MD studies of other engineered protein-based therapeutics, where it is normally possible to reach equilibrium within 100 ns, indicating excellent structural stability. The gradual decrease in SASA and replenishing radius of gyration pathways further affirm a compact, energetically preferable fold conformation, which confirms that the construct is properly folded and firmly bound to FGFR2 variants despite solvent and thermal disruptions (28). However, comparative benchmarking against native FGF10-FGFR complexes and FGF10-alone controls will be required in future computational and experimental studies to quantitatively determine whether fusion engineering alters receptor-binding performance relative to the native ligand.

Unlike earlier computational studies involving independent computational studies of individual functional AMPs or independent growth factors, the current study combines antimicrobial defense and regenerative signaling into a single biomolecule (42). Although cathelicidin-derived peptides have the potential to be used to speed up the repair of the epithelia, they are somehow structurally unstable in enzymatic environments, recombinant FGF2 can also repair it but this poses an infection risk because it lacks any antimicrobial coverage. Instead, our dual-functional construct, however, exhibits enhanced predicted stability, affinity to receptors and biosafety, which echoes new tendencies in next-generation biologics where the concept of multifunctional fusion proteins continues gaining momentum (43).

This study provides a detailed computational model of a dual-action fusion protein with the potential of preventing post-laser hemorrhoidal wound infection. The construct has good structural integrity, good receptor-binding energies, dynamic stability, and high biosafety profiles, which makes it an attractive therapeutic prototype that can be further validated empirically (44,45). Although the data available in silico are very promising, further in vitro expression and in vivo testing are required to determine biocompatibility, immunogenicity, antimicrobial activity, and wound -healing efficacy under controlled experimental settings. Future translational research will consider its possibility as a back-up therapeutic or adjunctive preventive during laser-based anorectal surgeries, and thus this may help fill the current gap between infection control and tissue repair.

Limitations

Although the computational results presented in this study indicate favorable predicted structural stability, solubility, and receptor interaction patterns, the proposed fusion construct remains an in-silico candidate and its therapeutic potential must be interpreted as hypothesis-generating. Molecular docking and molecular dynamics simulations provide predictive evidence of structural compatibility and interaction stability; however, they do not confirm biological activity, clinical efficacy, or therapeutic adequacy.

Importantly, the predicted outcomes cannot validate real antimicrobial performance against clinically relevant pathogens, nor can they confirm stimulation of epithelial repair, fibroblast proliferation, angiogenesis, or activation of downstream FGFR signaling pathways. In addition, computational biosafety screening tools such as AllerTOP and ToxiPred

provide probabilistic predictions and cannot replace experimental evaluation of allergenicity, toxicity, and immunogenicity.

Furthermore, the docking and MD simulation models do not fully account for complex physiological factors including post-translational modifications, proteolytic degradation, receptor dimerization dynamics, the influence of extracellular matrix components, or the polymicrobial wound microenvironment typical of post-laser anorectal wounds. Although the solubility and folding predictions suggest favorable recombinant expression potential, experimental confirmation is required through in vitro expression, purification, and structural validation. The docking and molecular dynamics analyses were not directly benchmarked against native ligand-receptor reference systems (e.g., the native FGF10-FGFR2b complex) or against FGF10 alone under identical computational settings. Therefore, the reported docking scores and stability metrics should be interpreted as predictive indicators of structural compatibility rather than as evidence of improved binding performance compared with native FGF10. Future work will include comparative docking/MD benchmarking and binding free energy calculations to quantitatively evaluate the engineered construct relative to native FGF-FGFR interactions.

In addition, biosafety predictions obtained from AllerTOP v2.0 and ToxiPred represent computational probability-based assessments and should not be interpreted as experimentally validated evidence of non-toxicity or non-allergenicity. Although these tools provide preliminary screening support, definitive evaluation of immunogenicity, cytotoxicity, and allergenic potential will require comprehensive in vitro and in vivo experimental validation. Therefore, the current construct should be regarded as a computational candidate pending future biosafety confirmation.

Therefore, future work will focus on recombinant production of the fusion protein followed by experimental validation using in vitro antimicrobial assays, cytotoxicity testing, receptor activation studies, and in vivo wound-healing models. These steps will be essential to confirm the translational potential of the proposed construct for preventing infection and supporting tissue repair in post-laser hemorrhoidal wounds.

Conclusion

This study illustrates the logical in silico pattern of an antimicrobial-growth factor fusion protein to eradicate infection and enhance tissue regeneration after laser treatment of hemorrhoidal disease. The resulting fusion construct comprising of four biocompatible antimicrobial peptide conjugation of the FGF10 region exhibited a strong physicochemical stability, retained structural integrity and suitable binding of FGFR2 isoforms. Good binding free energies, long-lasting (500 0ns) molecular dynamics simulations, and thermodynamic equilibrium were supported by the use of molecular docking and extended (500 0ns) molecular dynamics simulations and, thus, can support its potential as a stable, biologically viable therapeutic candidate. In comparison to the traditional monotherapeutic approaches, this engineered molecule has two functionality synergy: the antimicrobial peptides inhibit bacterial invasion, and the growth factor domain promotes the epithelial repair and angiogenesis. As a result, the proposed construct is a future-generation bioengineered therapeutic that can be used to treat infections, and heal wounds, at the same time. Its translational potential in clinical use in anorectal surgery will be further defined by future experimental validation, expression profiling and in vivo analyses.

Author Contributions

Study conception and design: **Özlem Karaca Ocak;** data collection: **Zoha Naeem;** analysis and interpretation of results: **Özlem Karaca Ocak, Zoha Naeem;** draft manuscript preparation: **Özlem Karaca Ocak.** The authors reviewed the results and approved the final version of the article.

Conflicts of Interest

The authors declare that there is no conflict of interest.

Financial Support

This study did not receive any financial support.

Ethical Approval

Ethics committee approval was not required because the study was conducted entirely using in-silico computational methods and did not involve human or animal subjects.

REFERENCES

1. Gallo G, Martellucci J, Sturiale A, Clerico G, Milito G, Marino F, et al. Consensus statement of the Italian society of colorectal surgery (SICCR): management and treatment of hemorrhoidal disease. Tech Coloproctol. 2020;24(2):145-164. https://doi.org/10.1007/s10151-020-02149-1
2. Rubbini M, Ascanelli S. Classification and guidelines of hemorrhoidal disease: Present and future. World J Gastrointest Surg. 2019;11(3):117-121. https://doi.org/10.4240/wjgs.v11.i3.117
3. Ray-Offor E, Amadi S. Hemorrhoidal disease: Predilection sites, pattern of presentation, and treatment. Ann Afr Med. 2019;18(1):12. https://doi.org/10.4103/aam.aam_4_18
4. Kaidar-Person O, Person B, Wexner SD. Hemorrhoidal disease: A comprehensive review. J Am Coll Surg. 2007;204(1):102-117. https://doi.org/10.1016/j.jamcollsurg.2006.08.022
5. Lie H, Zhang X, Chen Y, Li J, Wang L, Liu Y, et al. Laser hemorrhoidoplasty for hemorrhoidal disease: a systematic review and meta-analysis. Lasers Med Sci. 2022;37(9):3621-3630. https://doi.org/10.1007/s10103-022-03643-8
6. Wee IJY, Koo CH, Seow-En I, Ng YYR, Lin W, Tan EJKW. Laser hemorrhoidoplasty versus conventional hemorrhoidectomy for grade II/III hemorrhoids: a systematic review and meta-analysis. Ann Coloproctol. 2023;39(1):3-10. https://doi.org/10.3393/ac.2022.00598.0085

7. Maloku H, Gashi Z, Lazovic R, Islami H, Juniku-Shkololli A. Laser hemorrhoidoplasty procedure vs open surgical hemorrhoidectomy: a trial comparing 2 treatments for hemorrhoids of third and fourth degree. Acta Inform Med. 2014;22(6):365-367. https://doi.org/10.5455/aim.2014.22.365-367
8. Yu Q, Zhang Y, Li X, Wang H, Chen J, Liu L, et al. The beneficial effect of Sanhuang ointment and its active constituents on experimental hemorrhoids in rats. J Ethnopharmacol. 2024;319:117173. https://doi.org/10.1016/j.jep.2023.117173
9. Qie G, Wan M, Cui M, Xia W, Liu Q. Effect of active wound dressing on postoperative pain and wound healing in patients undergoing anorectal surgery. BMC Gastroenterol. 2025;25(1):320. https://doi.org/10.1186/s12876-025-03922-y
10. Büyükkiraz ME, Kesmen Z. Antimicrobial peptides (AMPs): A promising class of antimicrobial compounds. J Appl Microbiol. 2022;132(3):1573-1596. https://doi.org/10.1111/jam.15314
11. Huan Y, Kong Q, Mou H, Yi H. Antimicrobial peptides: classification, design, application and research progress in multiple fields. Front Microbiol. 2020;11:582779. https://doi.org/10.3389/fmicb.2020.582779
12. Adikusuma W, Pratama MR, Yusuf M, Santoso B, Rahmawati F, Kurniawan A, et al. Integrated genomic network analysis revealed potential of a druggable target for hemorrhoid treatment. Saudi Pharm J. 2023;31(12):101831. https://doi.org/10.1016/j.jsps.2023.101831
13. Ali N, Ahmad S, Asrar B, Khan M, Naveed M, Iqbal M, et al. Exploring nonstructural NS5B protein to design a multi-epitope-based vaccine against HCV: immuno-informatics approach. Silico Pharmacol. 2025;13(3):160. https://doi.org/10.1007/s40203-025-00448-9
14. Rao H, Kumar P, Sharma A, Singh R, Gupta D, Patel S, et al. In silico exploration of potential phytoconstituents from the bark extract of Boswellia serrata for hemorrhoidal disease: molecular docking and molecular dynamics analysis. Chem Biodivers. 2024;21(2):e202301416. https://doi.org/10.1002/cbdv.202301416
15. Jan A, Khan A, Ali N, Aslam S, Ahmad S, Naveed M, et al. Target-AMP: computational prediction of antimicrobial peptides by coupling sequential information with evolutionary profile. Comput Biol Med. 2022;151:106311. https://doi.org/10.1016/j.compbiomed.2022.106311
16. Dimitrov I, Flower DR, Doytchinova I. AllerTOP - a server for in silico prediction of allergens. BMC Bioinformatics. 2013;14(Suppl 6):S4. https://doi.org/10.1186/1471-2105-14-S6-S4
17. Mishra NK, Singla D, Agarwal S, Raghava GPS. ToxiPred: A server for prediction of aqueous toxicity of small chemical molecules in Tetrahymena pyriformis. J Transl Toxicol. 2014;1(1):21-27. https://doi.org/10.1166/jtt.2014.1005
18. Naveed M, Ahmad S, Ali N, Khan M, Asrar B, Iqbal M, et al. Computational design of a glycosylated multi-epitope vaccine against HAsV-1 and HAsV-2 astrovirus for acute gastroenteritis. Sci Rep. 2025;15(1):13954. https://doi.org/10.1038/s41598-025-96989-2
19. Artimo P, Jonnalagedda M, Arnold K, Baratin D, Csardi G, de Castro E, et al. ExPASy: SIB bioinformatics resource portal. Nucleic Acids Res. 2012;40(W1):W597-W603. https://doi.org/10.1093/nar/gks400
20. Hebditch M, Carballo-Amador MA, Charonis S, Curtis R, Warwicker J. Protein-Sol: a web tool for predicting protein solubility from sequence. Bioinformatics. 2017;33(19):3098-3100. https://doi.org/10.1093/bioinformatics/btx345
21. Li C, Zhang H, Wang Y, Liu J, Zhao X, Chen Z, et al. Design of a multi-epitope recombinant BCG vaccine targeting Brucella OMP31, LptE and VirB2 in immunoinformatics approaches. PLoS One. 2025;20(11):e0334843. https://doi.org/10.1371/journal.pone.0334843
22. Jumper J, Evans R, Pritzel A, Green T, Figurnov M, Ronneberger O, et al. Highly accurate protein structure prediction with AlphaFold. Nature. 2021;596:583-589. https://doi.org/10.1038/s41586-021-03819-2
23. Burley SK, Bhikadiya C, Bi C, Bittrich S, Chen L, Crichlow GV, et al. RCSB Protein Data Bank: powerful new tools for exploring 3D structures of biological macromolecules. Nucleic Acids Res. 2021;49(D1):D437-D451. https://doi.org/10.1093/nar/gkaa1038
24. Kozakov D, Hall DR, Xia B, Porter KA, Padhorny D, Yueh C, et al. The ClusPro web server for protein-protein docking. Nat Protoc. 2017;12(2):255-278. https://doi.org/10.1038/nprot.2016.169
25. Wallace AC, Laskowski RA, Thornton JM. LIGPLOT: a program to generate schematic diagrams of protein-ligand interactions. Protein Eng. 1995;8(2):127-134. https://doi.org/10.1093/protein/8.2.127
26. Alexander N, Woetzel N, Meiler J. Bcl::Cluster: a method for clustering biological molecules coupled with visualization in the PyMOL Molecular Graphics System. Proc IEEE ICCABS. 2011:13-18. https://doi.org/10.1109/ICCABS.2011.5729867
27. Bowers KJ, Chow E, Xu H, Dror RO, Eastwood MP, Gregersen BA, et al. Scalable algorithms for molecular dynamics simulations on commodity clusters. Proc SC. 2006:84. https://doi.org/10.1145/1188455.1188544
28. Albalawi IAA, Mirghani HO. The quality of life after trans oral video-assisted thyroidectomy and cervical thyroidectomy: a systematic review and meta-analysis. Front Surg. 2023;10:1116473. https://doi.org/10.3389/fsurg.2023.1116473
29. Harun H, Haroen H, Mirwanti R, Apriani N, Akuoko C. Uncovering the benefits of povidone iodine compared to other therapeutic agents in wound infection prevention and healing outcomes: a scoping review. J Multidiscip Healthc. 2024;17:3605-3616. https://doi.org/10.2147/JMDH.S469037
30. Memarbashi E, Nasiri-Formi E, Etezadpour M, Hosseinimehr SJ. Arnebia euchroma root ointment for post-hemorrhoidectomy wound care: a randomized controlled trial. Adv Integr Med. 2025;12(4):100576. https://doi.org/10.1016/j.aimed.2025.100576
31. Shityakov S, Lubinets NS, Skorb EV, Skurikhin EG, Kravtsov VY. Targeted anti-inflammatory effects of chloramphenicol via TLR4 inhibition in postoperative hemorrhoid treatment: a clinico-computational cohort study. Curr Med Chem. 2025;32. https://doi.org/10.2174/0109298673378981250710055128
32. Lei J, Sun L, Huang S, Zhu C, Li P, He J, et al. The antimicrobial peptides and their potential clinical applications. Am J Transl Res. 2019;11(7):3919-3931.
33. Lekhashree MG, Samhitha J. Evidence-led innovations and experimental approaches in hemorrhoid treatment. J Adv Med Pharm Res. 2025;6(2):127-142. https://doi.org/10.21608/jampr.2025.399256.1101

34. Arumugam S, Varamballi P. In-silico design of envelope based multi-epitope vaccine candidate against Kyasanur forest disease virus. Sci Rep. 2021;11:17118. https://doi.org/10.1038/s41598-021-94488-8

35. Naveed M, Ahmad S, Ali N, Khan M, Asrar B, Iqbal M, et al. Development of a novel multiepitope vaccine against Menangle virus using in-silico approaches by targeting its transmembrane proteins. Sci Rep. 2025;15(1):13715. https://doi.org/10.1038/s41598-025-98151-4

36. Asrar B, Ali N, Ali I, Naveed M. In silico investigation of ketamine and methylphenidate drug-drug conjugate for MDD and ADHD treatment using MD simulations and MMGBSA. Sci Rep. 2025;15:24565. https://doi.org/10.1038/s41598-024-82302-0

37. Bukhari SNA. Emerging nanotherapeutic approaches to overcome drug resistance in cancers with update on clinical trials. Pharmaceutics. 2022;14(4):866. https://doi.org/10.3390/pharmaceutics14040866

38. Dar HA, Zaheer T, Shehroz M, Ullah N, Naz K, Muhammad SA, et al. Multiepitope subunit vaccine design against COVID-19 based on the spike protein of SARS-CoV-2: an in silico analysis. J Immunol Res. 2020;2020:8893483. https://doi.org/10.1155/2020/8893483

39. Naveed M, Ahmad S, Ali N, Khan M, Asrar B, Iqbal M, et al. Designing a novel peptide-based multi-epitope vaccine to evoke a robust immune response against pathogenic multidrug-resistant Providencia heimbachae. Vaccines. 2022;10(8):1300. https://doi.org/10.3390/vaccines10081300

40. Asadollahi E, Zomorodipour A, Soheili ZS, Jahangiri B, Sadeghizadeh M. Development of a multi-neoepitope vaccine targeting non-small cell lung cancer through reverse vaccinology and bioinformatics approaches. Front Immunol. 2025;16:1521700. https://doi.org/10.3389/fimmu.2025.1521700

41. Gillett M, Dallosso HM, Dixon S, Brennan A, Carey ME, Campbell MJ, et al. Delivering the diabetes education and self management for ongoing and newly diagnosed programme for people with newly diagnosed type 2 diabetes: cost effectiveness analysis. BMJ. 2010;341:c4093. https://doi.org/10.1136/bmj.c4093

42. Shaon MSH, Hasan M, Rahman MS, Ahmed S, Islam M, Rahman MM, et al. AMP-RNNpro: a two-stage approach for identification of antimicrobials using probabilistic features. Sci Rep. 2024;14:12892. https://doi.org/10.1038/s41598-024-63461-6

43. Singh O, Hsu WL, Su ECY. Co-AMPpred for in silico-aided predictions of antimicrobial peptides by integrating composition-based features. BMC Bioinformatics. 2021;22:389. https://doi.org/10.1186/s12859-021-04305-2

44. Das NC, Gorai S, Gupta PSS, Panda SK, Rana MK, Mukherjee S. Immune targeting of filarial glutaredoxin through a multi-epitope peptide-based vaccine: a reverse vaccinology approach. Int Immunopharmacol. 2024;133:112120. https://doi.org/10.1016/j.intimp.2024.112120

45. Dobhal S, Sharma A, Singh P, Kumar V, Tiwari S, Singh R, et al. In silico identification of MHC displayed tumor associated peptides in ovarian cancer for multi-epitope vaccine construct. Endocr Metab Immune Disord Drug Targets. 2024;24(12):1401-1413. https://doi.org/10.2174/0118715303169428231205173914